Chinese Journal of Natural Medicines

**Maackiain inhibits proliferation and promotes apoptosis of nasopharyngeal carcinoma cells by inhibiting the MAPK/Ras signaling pathway**

Xing JIANG, Xiaonan YANG, Yanxia SHI, Yan LONG, Wenqing SU, Wendong HE, Kunhua WEI, Jianhua MIAO

**Citation:** Xing JIANG, Xiaonan YANG, Yanxia SHI, Yan LONG, Wenqing SU, Wendong HE, Kunhua WEI, Jianhua MIAO, Maackiain inhibits proliferation and promotes apoptosis of nasopharyngeal carcinoma cells by inhibiting the MAPK/Ras signaling pathway, Chinese Journal of Natural Medicines, 2023, 21(3), 185−196. doi: 10.1016/S1875−5364(23)60420−0.

View online: https://doi.org/10.1016/S1875−5364(23)60420−0

Available online at www.sciencedirect.com
ScienceDirect
*Chinese Journal of Natural Medicines* 2023, **21**(3): 185-196
doi: 10.1016/S1875-5364(23)60420-0
Chinese Journal of Natural Medicines

•Original article•

# Maackiain inhibits proliferation and promotes apoptosis of nasopharyngeal carcinoma cells by inhibiting the MAPK/Ras signaling pathway

JIANG Xing[1, 2, 3Δ], YANG Xiaonan[2Δ*], SHI Yanxia[1, 2], LONG Yan[1, 2], SU Wenqing[2, 4], HE Wendong[2, 5], WEI Kunhua[2], MIAO Jianhua[1, 2*]

[1] *College of Pharmacy, Guangxi Medical University, Nanning 530021, China;*
[2] *Guangxi Key Laboratory of Medicinal Resources Protection and Genetic Improvement/Guangxi Engineering Research Center of TCM Resource Intelligent Creation, Guangxi Botanical Garden of Medicinal Plants, Nanning 530023, China;*
[3] *The Second Affiliated Hospital, Hengyang Medical School, University of South China, Hengyang 421001, China;*
[4] *College of Pharmacy, Youjiang Medical University for Nationalities, Baise 533000, China;*
[5] *Department of Pharmacy, Guangxi Medical University Affiliated Tumor Hospital, Nanning 530021, China*

Available online 20 Mar., 2023

**[ABSTRACT]** Nasopharyngeal carcinoma (NPC) is the third most common malignancy with a high recurrence and metastasis rate in South China. Natural compounds extracted from traditional Chinese herbal medicines have been developed and utilized for the treatment of a variety of cancers with modest properties and slight side effects. Maackiain (MA) is a type of flavonoid that was first isolated from leguminous plants, and it has been reported to relieve various nervous system disorders and exert anti-allergic as well as anti-inflammatory effects. In this study, we demonstrated that MA inhibited proliferation, arrested cell cycle and induced apoptosis in nasopharyngeal carcinoma CNE1 and CNE2 cells *in vitro* and *in vivo*. The expression of the related proteins associated with these processes were consistent with the above effects. Moreover, transcriptome sequencing and subsequent Western blot experiments revealed that inhibition of the MAPK/Ras pathway may be responsible to the anti-tumor effect of MA on NPC cells. Therefore, the effects of MA and an activator of this pathway, tertiary butylhydroquinone (TBHQ), alone or combination, were investigated. The results showed TBHQ neutralized the inhibitory effects of MA. These data suggest that MA exerts its anti-tumor effect by inhibiting the MAPK/Ras signaling pathway and it has the potential to become a treatment for patients with NPC.

**[KEY WORDS]** Nasopharyngeal carcinoma; Maackiain; Proliferation; Cell cycle; Apoptosis; Transcriptome sequencing; MAPK/Ras signaling pathway

**[CLC Number]** R965 **[Document code]** A **[Article ID]** 2095-6975(2023)03-0185-12

## Introduction

Nasopharyngeal carcinoma (NPC) is a common malignancy originating in the epithelium of the nasopharynx [1]. In 2020, there were 133 354 new cases and 80 008 deaths from NPC worldwide, which accounted for 0.7% and 0.8% of all cancers, respectively. Over 70% of new cases were distributed in East and Southeast Asia, with a high incidence in South China [2]. Radiotherapy, especially intensity-modulated radiotherapy (IMRT), is the most widely used treatment modality for non-metastatic NPC, which was significantly related with better 5-year locoregional control and overall survival [3, 4]. However, despite recent advances in medical technology, as many as 20%–30% of NPC patients tend to develop localized recurrence and/or distant metastasis after treatment [5]. Therefore, exploring potential novel effective drugs is an urgent requirement for the treatment of NPC.

Due to their hypotoxicity and unique pharmacological activities, many natural ingredients extracted from traditional

**[Received on]** 10-Sep.-2022
**[Research funding]** This work was supported by the Independent Subject of Guangxi Key Laboratory of Medicinal Resources Protection and Genetic Improvement (No. KL2022ZZ01), Guangxi Innovation-Driven Development Project (No. GuiKe AA18242040), the National Key R&D Program of China (Nos. 2019YFC1711000 and 2019YFC1711008), the Innovation Team Project of Guangxi Botanical Garden of Medicinal Plant (No. GuiYaoChuang2019002), the Innovation and Demonstration of Guangxi Academician Workstation (No. 2021AV07007) and Government Guided Local Science and Technology Development Project (No. GuiKeZY 20198018).
**[*Corresponding author]** E-mails: nannangood33@163.com (YANG Xiaonan); mjh1962@vip.163.com (MIAO Jianhua)
[Δ]These authors contributed equally to this work.
These authors have no conflict of interest to declare.

Chinese folk herbs have been used for the treatment of various diseases. Maackiain (MA) is a type of flavonoid that exists in several herbs including *Sophora tonkinensis* [6-8], *Millettia speciosa* [9, 10] and *Sophora flavescens* [11, 12]. It has been reported to exert biological activities in multiple diseases, in addition to its traditional anti-bacterial [13] and anti-inflammatory [14, 15] roles. Recent research has revealed that MA can relieve the symptoms of Alzheimer disease, Parkinson's disease and depression by inhibiting the activity of monoamine oxidase B (MAO-B) [16]. MA has also been shown to preserve normal renal function by reducing oxidative stress as well as inflammation associated with type 2 diabetes [17]. In addition, it alleviates the symptoms of osteoclast-related disorders by dampening osteoclastogenesis [18] and exerts protective effect against sepsis by activating the AMPK/Nrf2/HO-1 pathway [19].

Accumulating evidence indicates that MA may be a potential anti-tumor compound. For example, MA is the vital ingredient of the botanical drug, antitumor B (ATB) [20] and can induce the apoptosis of HL-60 leukemia cells [21]. MA also exerts anti-cancer effect in triple negative breast cancer cells [22]. However, the effect of MA on NPC, as well as its mechanisms has not been clearly understood. In this study, the effect of MA on the proliferation, cell cycle and apoptosis of NPC cells were explored both *in vitro* and *in vivo*. The results showed that MA is an excellent anti-NPC agent. Then, the underlying mechanism was investigated, which suggested that MA maybe a suppressant of the MAPK/Ras signaling pathway. In addition, tertiary butylhydroquinone (TBHQ) [23-25], a known MAPK/Ras pathway activator was found to reverse the anti-tumor effect of MA.

## Materials and Methods

### *Cell culture and reagents*

Human NPC cell lines, CNE1, CNE2 and immortalized normal nasopharyngeal epithelial NP69 cells were purchased from the Cell Bank of Central South University, Changsha, China. All NPC cells were cultured in Roswell Park Memorial Institute 1640 (RPMI-1640) medium supplemented with 10% fetal bovine serum (FBS). NP69 cells were cultured in keratinocyte medium (KM) with addition of a keratinocyte growth supplement (KGS, #2152). All the cells were incubated at 37 °C in a humidified atmosphere of 5% (*V*/*V*) $CO_2$. MA was purchased from Biopurify (China, #BP0907) and dissolved in DMSO prior to use.

### *Cell counting kit-8 assay*

CNE1 and CNE2 cells were seeded in 96-well plates at a density of 3000 cells/well. After incubation for 24 h, the cells were treated with indicated concentrations of MA (0, 20, 40, 60, 80 and 100 μmol·L$^{-1}$), and then cultured for another 24, 48 and 72 h. Subsequently, 10 μL CCK-8 reagent (Dojindo, Japan, #CK04) was added to each well before incubation at 37 °C for additional 2 h. The absorbance was measured on a microplate reader (TECAN, Switzerland) at 450 nm.

### *Ethynyl-2-deoxyuridine assay*

An ethynyl-2-deoxyuridine (EdU) cell proliferation assay kit (Sangon Biotech, Shanghai, China) was used to evaluate the effect of MA on cell proliferation. In brief, NPC cells ($5 \times 10^4$) were seeded into 24-well plates and treated with different concentrations of MA (0, 5, 10 and 20 μmol·L$^{-1}$). After incubation for 24 h, 10 μmol·L$^{-1}$ EdU solution was added and the cells were incubated at 37 °C in an atmosphere of 5% $CO_2$ for another 2 h. After washing and fixation, the cells were stained with TAMRA and Hoechst 33342 dyes. Images were captured by an inversed fluorescent microscope (Olympus, Tokyo, Japan). The number of EdU-positive cells were counted using ImageJ software.

### *Cell cycle and apoptosis assay*

The cell cycle was assessed using a PI/RNase staining buffer solution (BD Biosciences, USA, #550825) according to the manufacturer's instructions. The cells ($3 \times 10^5$) were seeded on 6-well plates and then subjected to corresponding treatments. Next, the cells were collected, fixed at −20 °C in 70% ethanol overnight and then washed twice with pre-cooled PBS. After re-suspending in 500 μL of PI/RNase staining buffer, the cells were incubated at room temperature for 30 min. The cell cycle was determined by a flow cytometer (BD Accuri™ C6, Piscataway, NJ, USA) and the results were analyzed with Modfit LT 4.1 software.

An Annexin V FITC Apop Dtec Kit I (BD Biosciences, USA, #556547) was used to determine the effect of MA on cell apoptosis. Briefly, the cells were treated with MA (0, 20, 40, 80 μmol·L$^{-1}$) for 24 h. Then, the cells were re-suspended in 1 × binding buffer and incubated with 5 μL of Annexin V-PE and 5 μL of 7-AAD in the darkness for 15 min. The stained cells were assessed by a flow cytometer (EMD Millipore Guava Easy Cyte Accuri C6, USA) and FlowJo 7.6 software was used for data analysis.

### *Western blot analysis*

Total cellular protein was extracted with cell lysis buffer (Beyotime, China, #P0013) containing phosphatase and proteinase inhibitors. A BCA protein assay kit (Beyotime, China, #P0011) was utilized to determine protein concentrations. Protein samples (30–60 μg) were separated by 12.5% SDS-PAGE (EpiZyme, China, #P0011) and transferred onto PVDF membrane (Millipore, Ireland, #ISEQ00010). The membrane was blocked with 5% skimmed milk for about 2 h, before incubation with appropriate primary antibodies at 4 °C overnight followed by HRP-labeled secondary antibodies (Beyotime, China, #A0208). The blots were visualized by BeyoECL Plus (Beyotime, China, #P0018S) and photographed by the ChemiDocTM MP Imaging System (BIORAD, USA, #12003154). The grey scale values were quantified by Image Lab 6.0 software.

The primary antibodies used in this study were purchased from Cell Signaling Technology: Proliferating Cell Nuclear Antigen (PCNA) (D3H8P) XP® rabbit mAb (1∶1000, #13110S), Cyclin D1 (92G2) rabbit mAb (1∶1000, #2978S), CDK4 (D9G3E) rabbit mAb (1∶1000,

#12790S), CDK6 (D4S8S) rabbit mAb (1 ∶ 1000, #13331S), P16 INK4A (E6N8P) rabbit mAb (1 ∶ 1000, #18769S), P21 Waf1/Cip1 (12D1) rabbit mAb (1 ∶ 1000, #2947S), B-cell lymphoma-2 (Bcl-2) (D55G8) rabbit mAb (1 ∶ 800, #4223S), Bax (D2E11) rabbit mAb (1 ∶ 1000, #5023S), Caspase-3 (D3R6Y) Rabbit mAb (1 ∶ 800, #14220S), cleaved Caspase-3 (Asp175) antibody (1 ∶ 800, #9661S), poly ADP-ribose polymerase (PARP) (46D11) rabbit mAb (1 ∶ 1000, #9532S), *β*-actin (13E5) rabbit mAb (1 ∶ 1000, #4970S), c-Raf antibody (1 ∶ 1000, #9422T), phospho-c-Raf (Ser259) antibody (1 ∶ 1000, #9421T), mitogen-activated protein kinase kinase (MEK) 1/2 (D1A5) rabbit mAb (1 ∶ 1000, #8727T), phospho-MEK1/2 (Ser217/221) (41G9) rabbit mAb (1 ∶ 1000, #9154T), P44/42 MAPK (Erk1/2) (137F5) rabbit mAb (1 ∶ 1000, #4695T) and phospho-p44/42 MAPK (Erk1/2) (Thr202/Tyr204) (D13.14.4E) XP® rabbit mAb (1 ∶ 1000, #4370T).

*RNA-sequence and KEGG pathway enrichment analysis*

Total cellular RNA was extracted by a TransZol Up Plus RNA Kit (Transgen, China, #ER501). RNAs were quantified using both a NanoDrop 2000 spectrophotometer and agarose gel electrophoresis. A MGIEasy RNA Library Prep Kit (Mgi Tech, China, #1000005276) was used to construct mRNA libraries and 1 μg of total RNA per sample was used for cDNA synthesis. The cDNA was then attached to an adapter after the ends were repaired and then inserted with a polyA tail. A BGISEQ-500RS genome sequencer and the BGISEQ-500RS high-throughput sequencing kit (Mgi Tech, China, #940-10037-00) were utilized for double-terminal sequencing with a 100 bp read length. The sequenced raw data were collected, while FastQC [26] and Trimmomatic [27] were used for quality control. Differential expressed genes (DEGs) were obtained after alignment and transcript assembly. The DEGs were then imported in order to perform KEGG pathway enrichment analysis.

*In vivo experiments*

Briefly, male athymic Balb/c nude mice (4−5 weeks, 18−21 g) were purchased from the Animal Laboratory Center of Guangxi Medical University. The animals were acclimated in a SPF-free barrier system for one week. Then, CNE1 or CNE2 cells ($1 \times 10^6$ cells suspended in 0.1 mL PBS) were subcutaneously injected into the right flank of each mouse. Tumor size was monitored with calipers every other day and the volume ($V$) was calculated according to following equation: $V$ = length × width$^2$ × π/6. Once the tumor volume reached 80−120 mm$^3$, the mice were randomly divided into three groups ($n$ = 5): a control (0.2 mL normal saline) group, a MA (20 mg·kg$^{-1}$) treatment group and a cisplatin (5 mg·kg$^{-1}$) treatment group. Normal saline or the corresponding drugs were intra-peritoneally injected every two days for 14 d. The mice were then sacrificed by cervical dislocation and tumor tissues were collected and weighed. In addition, the liver and kidneys as well as parts of tumor tissues were fixed with 4% paraformaldehyde for hematoxylin–eosin (H&E) staining and immunohistochemical (IHC) analysis. The animal study protocol was approved by the Ethics Committee of Guangxi Botanical Garden of Medicinal Plants (GXBGMP-20211201, Dec. 16th, 2021).

*H&E staining and IHC analysis*

The liver, kidney and tumor samples were fixed in 4% paraformaldehyde, embedded in paraffin and sliced into 4 μm sections. After dewaxing with xylene and hydrated with gradient alcohol, the sections were stained with hematoxylin and eosin (H&E) staining solutions. For immunohistochemistry (IHC) analysis, the paraffin-embedded sections were heated in an antigen-retrieval buffer bath at 95 °C for 20 min and blocked with 5% BSA at room temperature for 30 min, before incubation with primary antibodies against ki67 (1 ∶ 300, Abcam, #ab16667), cleaved caspase-3 (1 ∶ 300, Cell Signaling Technology, #9661S) and phospho-Erk1/2 (1 ∶ 200, Cell Signaling Technology, #4370T) at 4 °C overnight and subsequently with secondary antibody at 37 °C for 30 min the next day. The sections were then incubated with diaminobezidin (DAB) and counterstained with haematoxylin. At last, the sections were observed under an inverted light microscope.

*Statistical analysis*

Statistics analysis was performed by IBM SPSS Statistics 24.0 software. Two-tailed Student's *t*-tests or one-way ANOVA were used to evaluate the significant differences of experimental data between two groups. Data are represented as the means ± standard deviations (SDs). $P < 0.05$ was considered to be statistically significant.

## Results

*MA inhibited the proliferation of NPC cells*

In order to explore the effect of MA (Fig. 1A) on NPC cell lines, CNE1 and CNE2 cells were treated with various concentrations of MA (0, 20, 40, 60, 80 and 100 μmol·L$^{-1}$) for 24, 48 and 72 h. Then, CCK-8 assay was used to assess cell viability. The results indicated that MA inhibited the proliferation of CNE1 and CNE2 cells in a dose- and time-dependent manner (Figs. 1C and 1D). The $IC_{50}$ values of MA were 116.65 ± 3.05, 41.71 ± 2.16 and 20.28 ± 1.18 μmol·L$^{-1}$ in CNE1 cells and 80.28 ± 3.81, 25.14 ± 2.13 and 16.36 ± 0.47 μmol·L$^{-1}$ in CNE2 cells at 24, 48 and 72 h, respectively. However, the viability of immortalized normal nasopharyngeal epithelial NP69 cells was much less affected by similar concentrations of MA (Fig. 1B). Their IC50 values were 347.33 ± 35.76, 248.10 ± 28.31 and 166.48 ± 9.54 μmol·L$^{-1}$ at 24, 48 and 72 h, respectively.

Furthermore, EdU assay confirmed that MA significantly inhibited NPC cell proliferation at the concentrations of 5, 10 and 20 μmol·L$^{-1}$ (Figs. 1E and 1F). These results demonstrated that MA exerted obvious anti-tumor effect against NPC cells, with little toxicity to normal cells.

*MA arrested NPC cells at $G_0/G_1$ phase*

To further explore the inhibitory mechanism of MA on cell proliferation, flow cytometry (PI staining) was used to assess the phases of cell cycle distribution after treatment

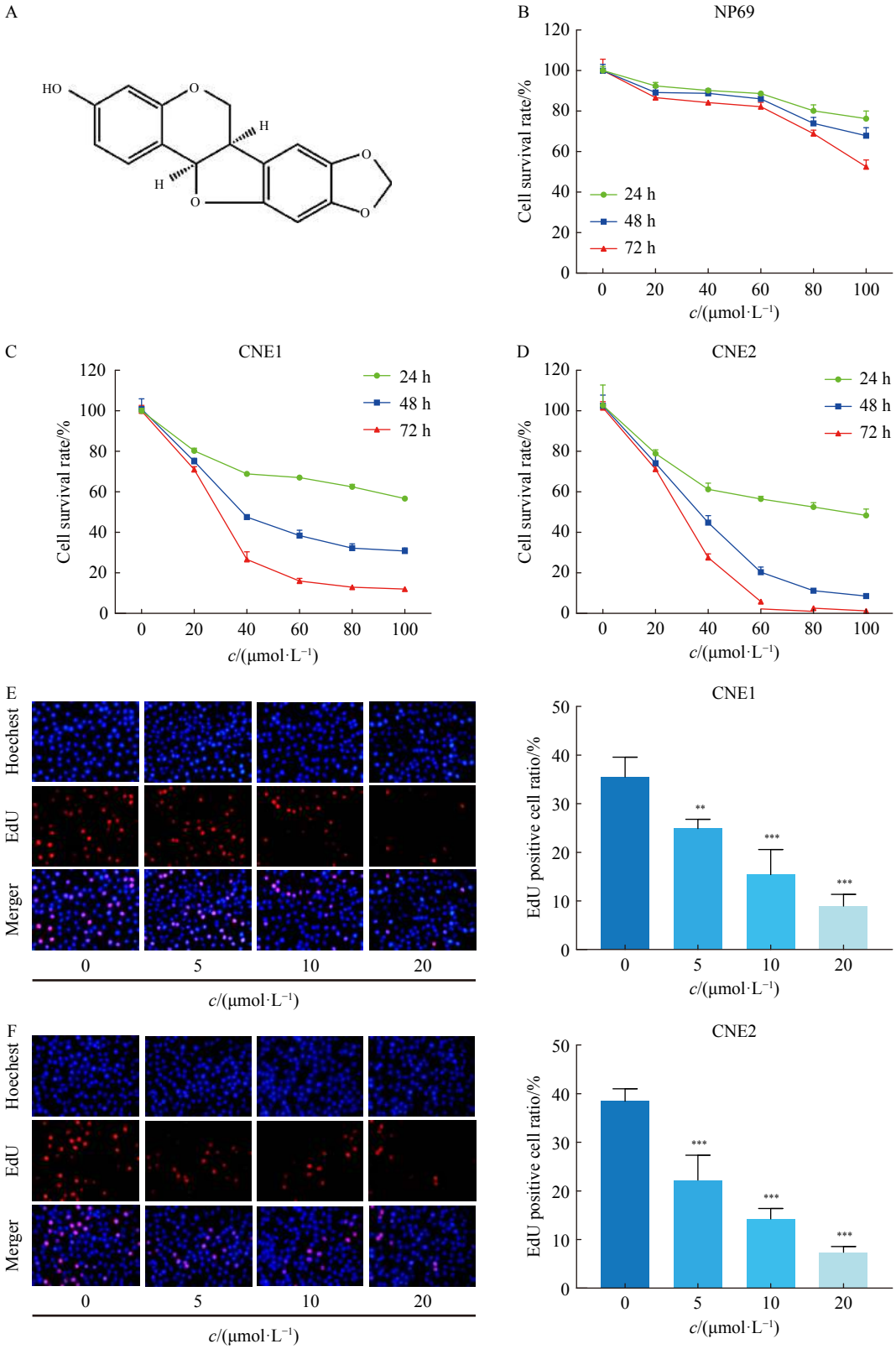


**Fig. 1 The anti-proliferative activities of MA in CNE1 and CNE2 cells. (A) The chemical structure of MA. (B) Effect of MA on the cell viability of normal nasopharyngeal epithelial NP69 cells. (C, D) The viability of CNE1 and CNE2 cells were significantly reduced after MA treatment. (E, F) The proliferation of CNE1 and CNE2 cells was inhibited after incubation with various concentrations of MA for 24 h. $^{**}P < 0.01$, $^{***}P < 0.001$ *vs* the negative control group. Data are presented as mean ± SD ($n = 3$).**

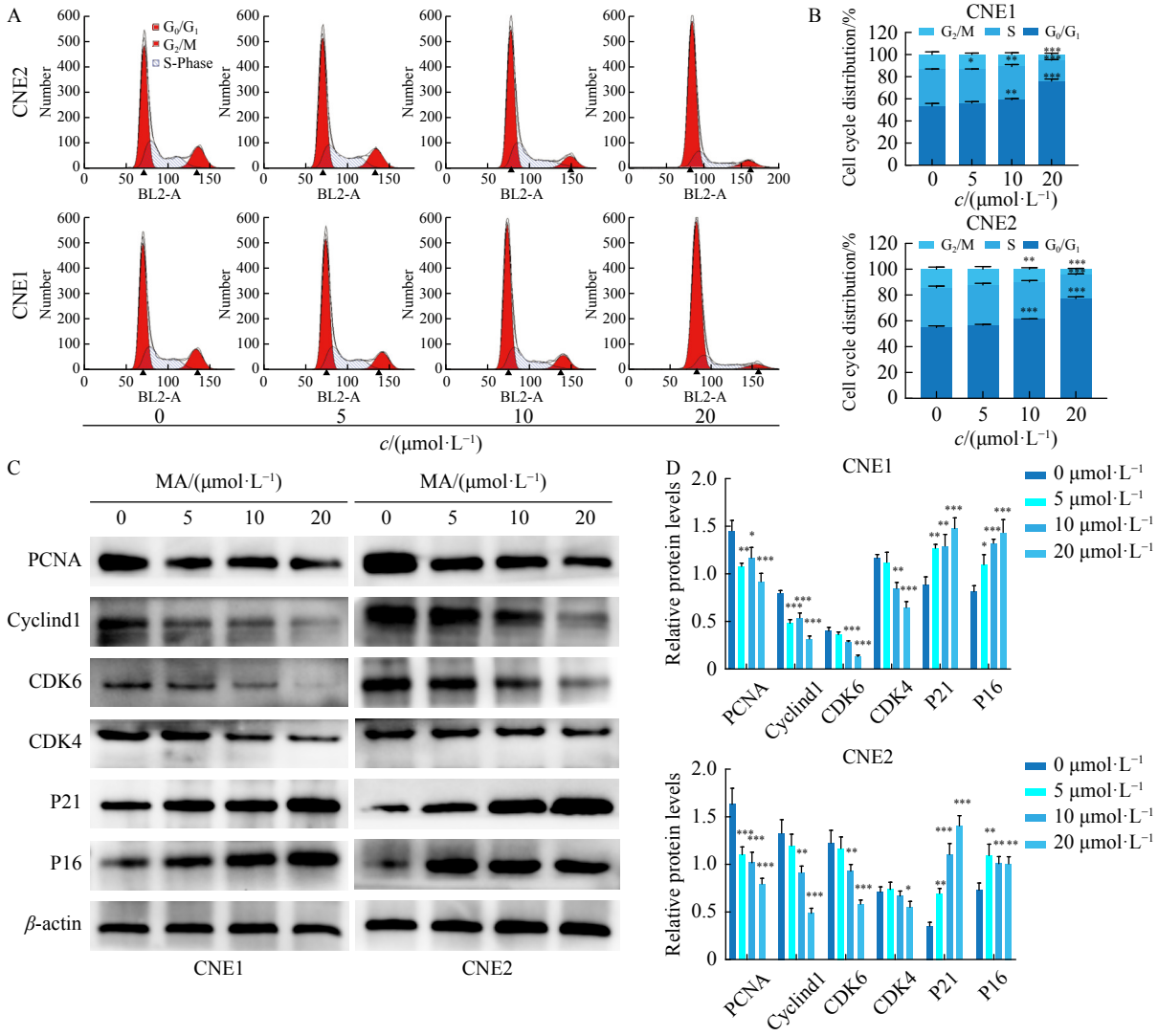


**Fig. 2 MA arrested cell cycle at $G_0/G_1$ phase in CNE1 and CNE2 cells. (A, B) Representative flow cytometry histograms showing the cell cycle distribution of CNE1 and CNE2 cells after treatment with MA for 24 h; (C, D) The expression of proliferation- and $G_0/G_1$-related biomarkers, PCNA, Cyclin D1, CDK6, CDK4, P21 and P16 was measured by Western blot after CNE1 and CNE2 cells were incubated with MA for 24 h. $^{*}P < 0.05$, $^{**}P < 0.01$, $^{***}P < 0.001$ *vs* the negative control group. Data are presented as mean ± SD ($n = 3$).**

with different concentrations of MA for 24 h. As shown in Figs. 2A and 2B, MA significantly increased the number of both CNE1 and CHE2 cells at $G_0/G_1$ phase ($P < 0.05$) at 10 and 20 μmol·L$^{-1}$. Moreover, the impact of MA on the biochemical regulators of cells at $G_0/G_1$ phase was confirmed by Western blot analysis. As shown in Figs. 2C and 2D, MA dose-dependently downregulated the expression of PCNA, CDK6, CDK4 and Cyclin D1 and upregulated the expression of P21 and P16 in both cell lines.

*MA induced the apoptosis of NPC cells*

Activation of cancer cell apoptosis is considered to be a vital mechanism for many chemotherapeutic agents. Therefore, after treatment with various concentrations of MA (0, 20, 40 and 80 μmol·L$^{-1}$) for 24 h, the apoptosis of CNE1 and CNE2 cells was measured by flow cytometry with annexin-V PE/7-AAD double staining (Fig. 3A). The number of apoptotic cells was 6.21%, 8.73%, 15.93% and 28.70% in CNE1 cells, while 6.79%, 10.73%, 24.50% and 30.10% in CNE2 cells after treatment with 0, 20, 40 and 80 μmol·L$^{-1}$ of MA, respectively (Fig. 3B). Furthermore, Western blot was performed to evaluate the effect of MA on several apoptosis-related biomarkers. As shown in Figs. 3C and 3D, MA increased the ratios of BAX/Bcl-2, cleaved caspase-3/total caspase-3 and cleaved PARP/total PARP in a dose-dependent manner in both cell lines.

*Transcriptome sequencing and KEGG pathway enrichment analysis*

Transcriptome sequencing was conducted to explore the mechanism associated with inhibited proliferation and promoted apoptosis in NPC cells caused by MA. CNE1 cells were treated with 10 μmol·L$^{-1}$ of MA or an equal aliquot of DMSO as a negative control for 24 h, and then total RNA

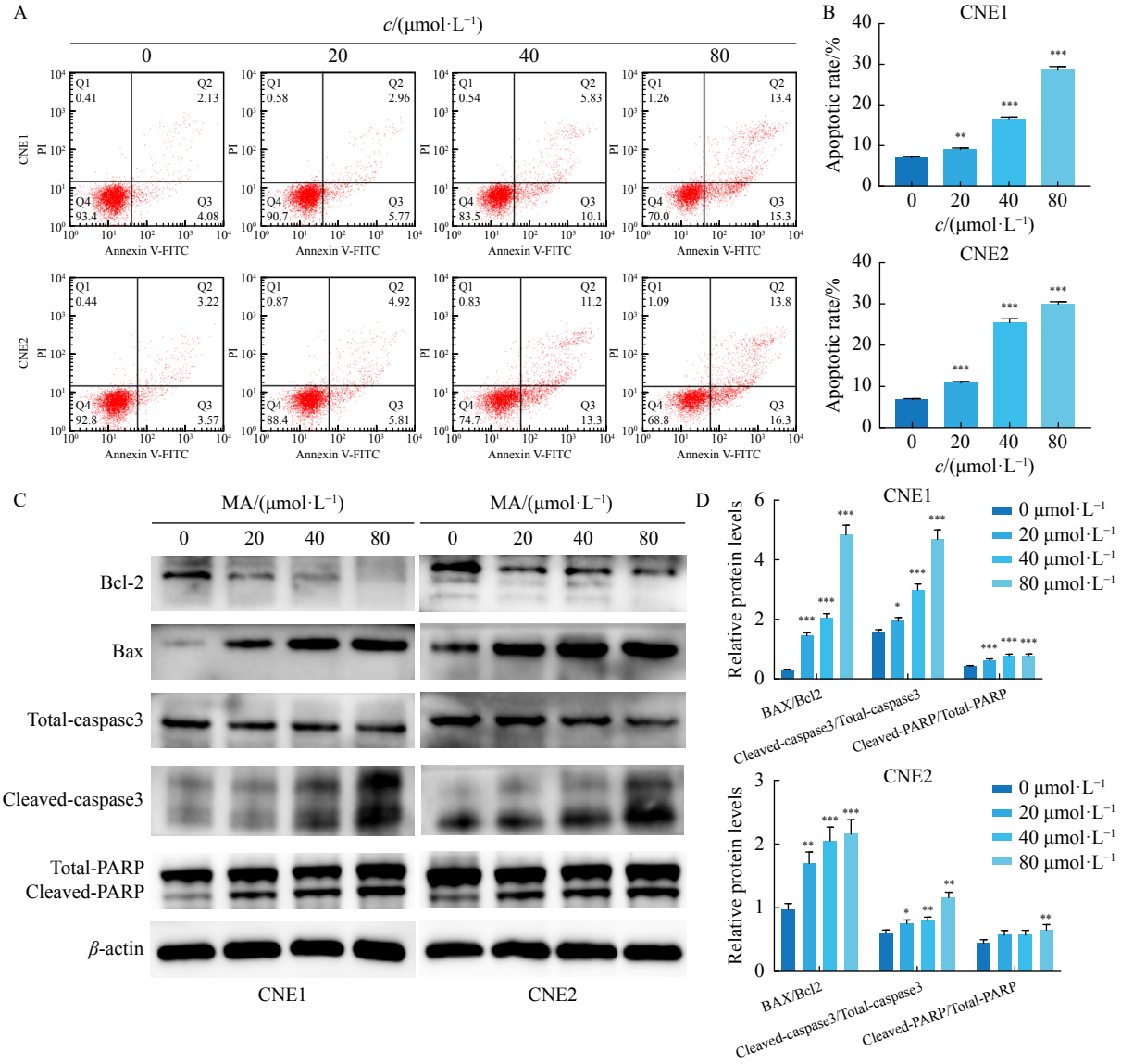


**Fig. 3 MA induced apoptosis in CNE1 and CNE2 cells. (A, B) The number of apoptotic cells was measured by flow cytometry after CNE1 and CNE2 cells were incubated with MA for 24 h. (C, D) The expression of apoptosis-related markers Bcl2, Bax, caspase-3 and PARP was measured by Western blot after CNE1 and CNE2 cells were incubated with MA for 24 h. $^{*}P < 0.05$, $^{**}P < 0.01$, $^{***}P < 0.001$ *vs* the negative control group. Data are presented as mean ± SD ($n = 3$).**

was extracted and sequenced. The DEGs found were presented as a volcano plot (Fig. 4A), where 553 up-regulated and 375 down-regulated genes were identified as having a |log2FC| greater than 1.0 and $P$ value < 0.05. KEGG enrichment analysis showed that the DEGs were mainly enriched in the MAPK, PI3K-Akt, Ras and Rap1 signaling pathways as well as in viral carcinogenesis (Fig. 4B). It is worth noting that most of the differential genes enriched in the MAPK signaling pathway had a lower $P$ value. In addition, there was overlap between the MAPK and Ras signaling pathways, which suggested the involvement of these pathways in the anti-tumor property of MA. To further confirm this hypothesis, the key proteins related to the MAPK/Ras signaling pathway were examined by Western blot. As shown in Figs. 4C and 4D, MA inhibited the phosphorylation of the downstream regulators of MAPK/Ras, namely Raf, MEK1/2 and Erk1/2, in a dose-dependent manner.

*MA regulated NPC progression via the MAPK/Ras signaling pathway*

Previous experiments showed that MA played an anti-tumor role by inhibiting cell proliferation, arresting cell cycle and promoting apoptosis *in vitro*. Moreover, the MAPK/Ras signaling pathway was blocked by MA. In order to explore whether the MAPK/Ras signaling pathway was necessary for MA to regulate NPC progression, CCK-8 and EdU assays as well as Western blot and flow cytometry were performed in the presence of TBHQ, a known MAPK/Ras signaling pathway activator. As shown in Figs. 5A–5D, TBHQ partially reversed the anti-proliferation, cell cycle arrest and pro-apoptotic effects of MA in CNE1 and CNE2 cells. These results

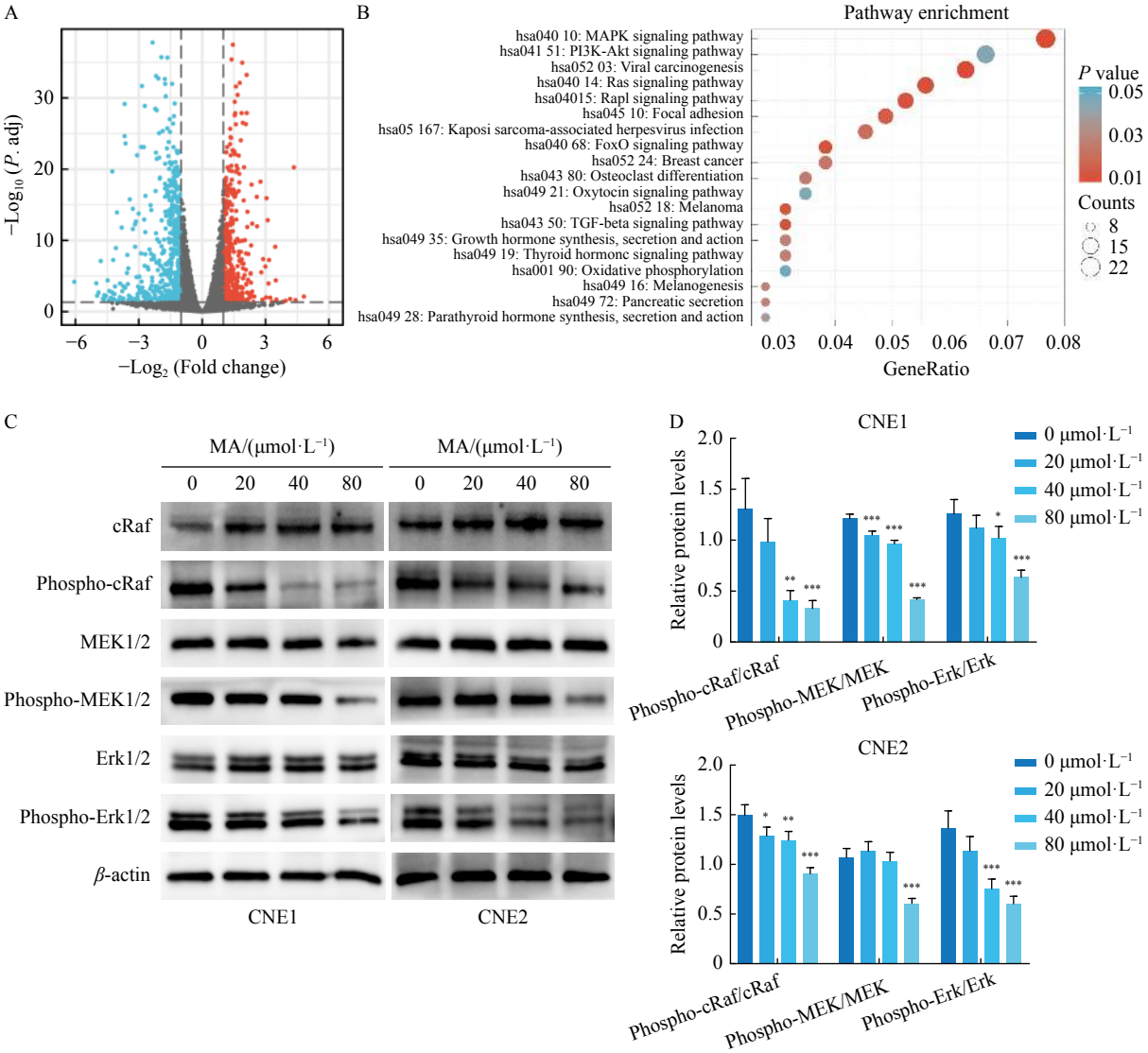


**Fig. 4 MA regulated the MAPK/Ras pathway in CNE1 and CNE2 cells. (A) A volcano plot for differentially expressed genes. The horizontal axis represents the fold change, and the vertical axis represents the adjusted p-value. The red, green and gray dots represent genes that are upregulated, downregulated and indifferent, respectively. (B) A bubble diagram illustrating the top 19 enriched pathways. (C, D) The expression of MAPK/Ras signaling pathway-related key proteins, cRaf, MEK1/2, Erk1/2 and their phosphorylation levels were investigated by Western blot. $^{*}P < 0.05$, $^{**}P < 0.01$, $^{***}P < 0.001$ *vs* the negative control group. Data are presented as mean ± SD ($n = 3$).**

were further confirmed by Western blot analysis. In the presence of TBHQ, the levels of PCNA, Cyclin D1, CDK6 and CDK4 were significantly higher than those in the MA group (Fig. 5E). In both two cell lines, the ratio of cleaved caspase-3/total caspase-3 in combination groups remarkably decreased, while a similar change was observed for the ratio of Bax/Bcl-2 in the combination group of CNE2 cells. Although there was no significant change in Bax/Bcl-2 ratio in the presence of MA or combination in CNE1 cells, the expression of the anti-apoptotic protein, Bcl-2, was higher in the combination group (Fig. 5F). Importantly, MA inhibited the phosphorylation of downstream proteins of the MAPK/Ras signaling pathway, which was reversed by TBHQ treatment (Fig. 5G).

*MA exerted antitumor effect in vivo*

To further investigate the effects of MA on NPC cells *in vivo*, Balb/c nude mice bearing CNE1 and CNE2 xenograft tumors were treated with MA (20 mg·kg$^{-1}$), with cisplatin (5 mg·kg$^{-1}$) as a positive control and normal saline (0.2 mL) as a negative control. As shown in Fig. 6A, the tumors in the MA and cisplatin groups were smaller than those in the control group. MA treatment significantly decreased the weight of CNE1 and CNE2 tumors by 30.62% ($P < 0.05$) and 38.99% ($P < 0.05$), and reduced the volume of CNE1 and CNE2 tumors by 29.19% ($P < 0.05$) and 26.86% ($P < 0.01$), respectively, compared with the control group. In addition, there was no significant difference in tumor weight and volume inhibition rate between the MA and cisplatin groups (Figs. 6B and

6C). Moreover, the body weight curves among the three groups were almost perfectly consistent (Fig. 6D). H&E staining revealed that some morphological changes related to cell apoptosis, including cell shrinkage and condensed nuclei

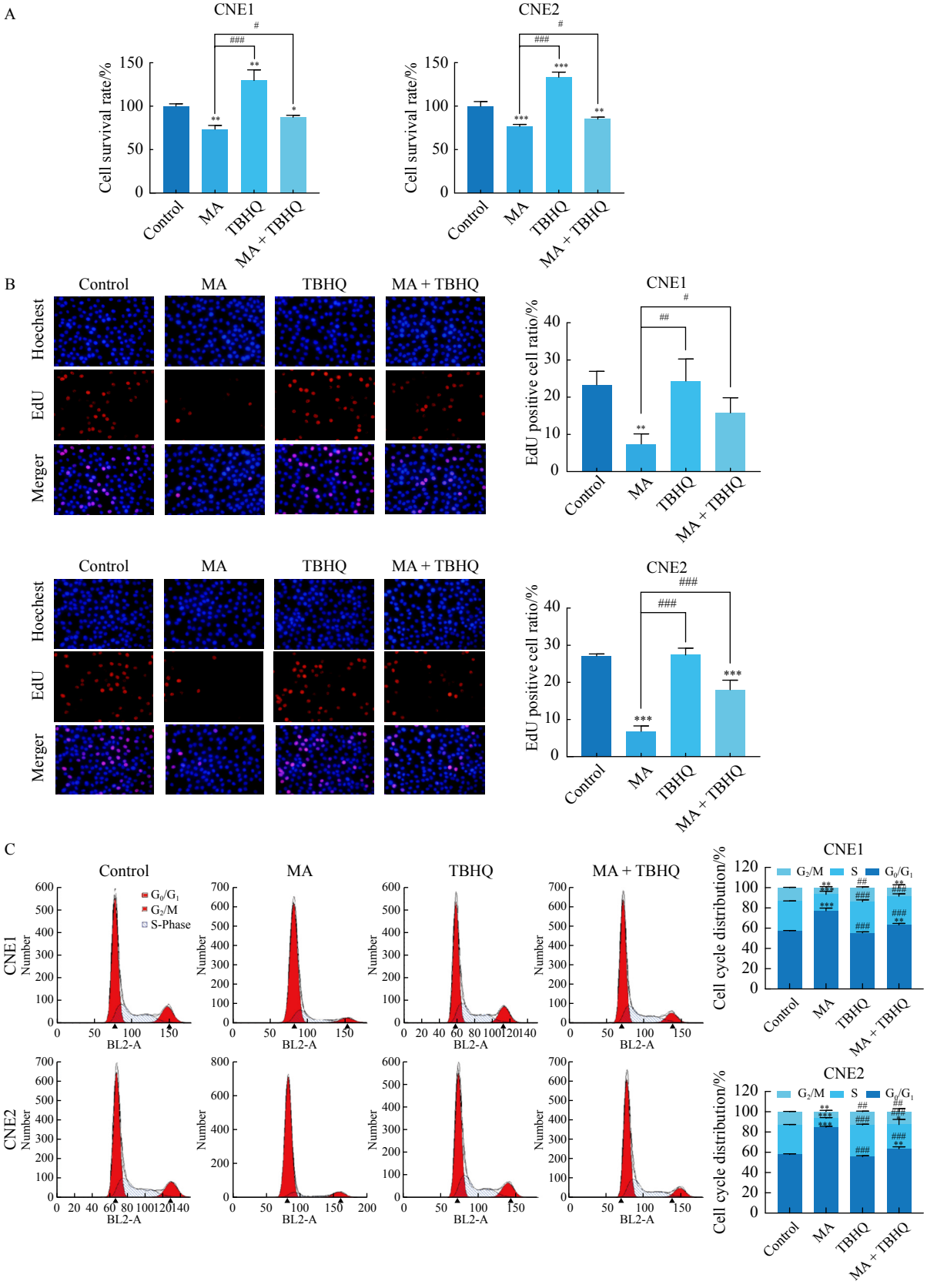

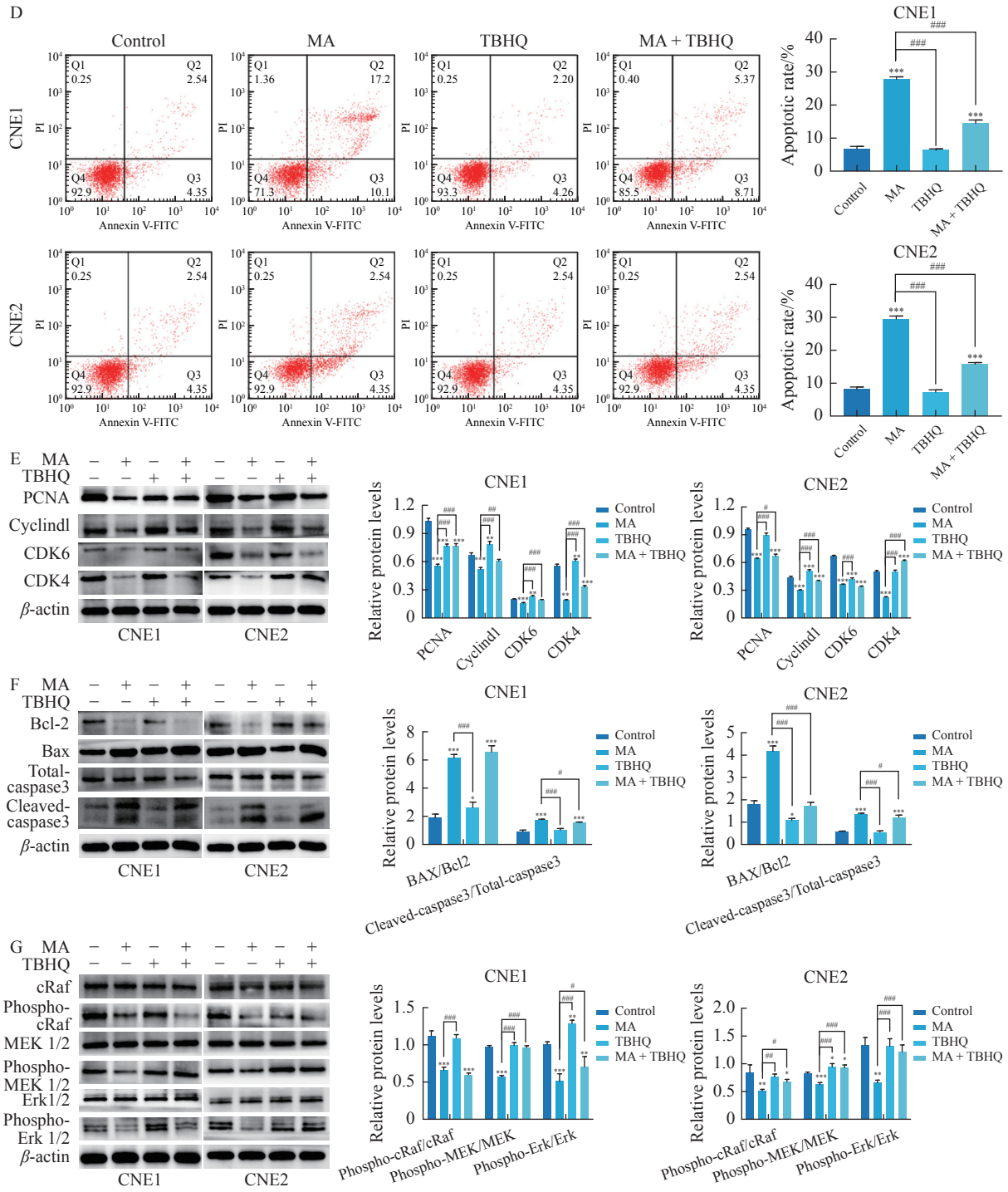


**Fig. 5 The MAPK/Ras signaling pathway was the target of MA. (A) The viability of CNE1 and CNE2 cells was measrued by CCK8 assay after incubation with MA (40 μmol·L$^{-1}$), TBHQ (10 μmol·L$^{-1}$) or both for 24 h. (B) The viability of CNE1 and CNE2 cells was detected by EdU assay after incubation with MA (20 μmol·L$^{-1}$), TBHQ (5 μmol·L$^{-1}$) or both for 24 h. (C, E) The cell cycle distribution and related protein expression of CNE1 and CNE2 cells after incubation with MA (20 μmol·L$^{-1}$), TBHQ (5 μmol·L$^{-1}$) or both for 24 h. (D, F) The cell apoptosis and expression of apoptotic markers of CNE1 and CNE2 after incubation with MA (80 μmol·L$^{-1}$), TBHQ (10 μmol·L$^{-1}$) or both for 24 h. (G) The expression of MAPK/Ras signaling pathway-related key proteins, cRaf, MEK1/2 and Erk1/2 and their phosphorylation levels were assessed by Western blot after CNE1 and CNE2 cells were incubated with MA (80 μmol·L$^{-1}$), TBHQ (10 μmol·L$^{-1}$) or both for 24 h. $^{*}P < 0.05$, $^{**}P < 0.01$ and $^{***}P < 0.001$ *vs* the control group; $^{\#}P < 0.05$, $^{\#\#}P < 0.01$ and $^{\#\#\#}P < 0.001$ *vs* the MA group. Data are presented as mean ± SD ($n = 3$).**

in tumor tissues, were more likely to be observed in the MA and cisplatin groups, although no significant changes in the liver and kidney tissues were seen (Fig. 6E). Furthermore, some key markers associated with cell proliferation, apoptos-

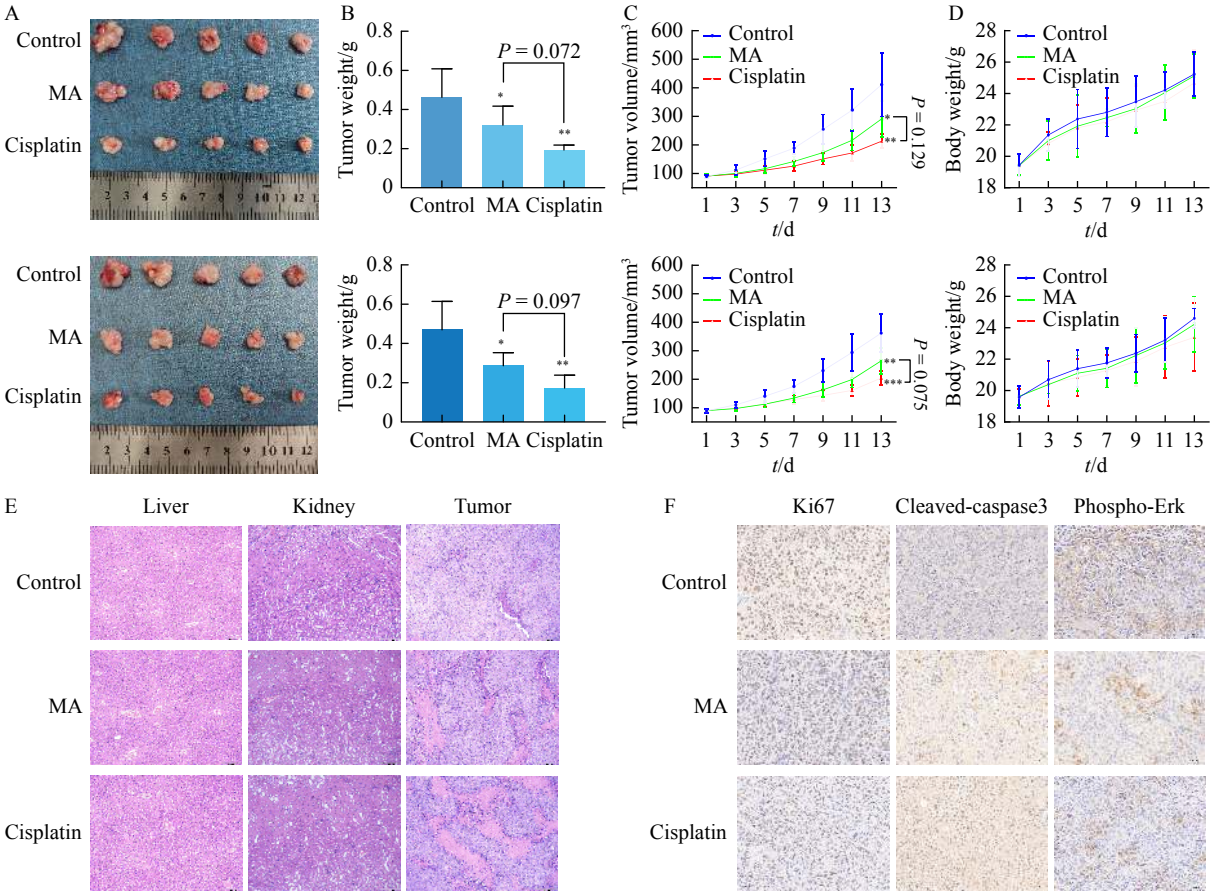


**Fig. 6 MA inhibited the growth of NPC *in vivo*. (A) Photographs of tumors from xenograft mice at the experimental end point ($n$ = 5). (B) The tumor weights of each group at the experimental end point ($n$ = 5). (C) Tumor growth curves of each group ($n$ = 5). (D) Body weight curves of each group ($n$ = 5). (E) Tumor, liver and kidney tissues in CNE1 xenograft tumor were observed by H&E staining (100 × ). (F) The expression of ki67, cleaved caspase-3 and phospho-Erk in CNE1 xenograft tumors were assessed by immunohistochemistry (400 × ). $^{*}P < 0.05$, $^{**}P < 0.01$, $^{***}P < 0.001$ *vs* the negative control group. Data are presented as mean ± SD ($n$ = 5)**

is and the MAPK/Ras signaling pathways were examined by immunohistochemistry staining. As shown in Fig. 6F, the expression of ki67 and phospho-Erk1/2 were lower in the MA group, although MA increased the expression of cleaved caspase-3. These results demonstrated that MA inhibited proliferation and promoted apoptosis of NPC *via* the MAPK/Ras signaling pathways *in vivo*, which was in accordance with the *in vitro* data.

## Discussion

NPC is a malignant head and neck carcinoma arising from the epithelium of the nasopharynx. The morbidity associated with NPC in the population of South China is about 2–10/100 000, which is significantly higher than those in Caucasians [28]. As NPC often infiltrates and is often in close proximity to critical organs and tissues, such as the brain stem cell area, optic nerves and main blood vessels, surgery and radiotherapy are not often used for the treatement NPC [29]. Although recent years saw significant improvement in radiotherapy, approximately 20%–30% of NPC patients may still suffer from local recurrence and distant metastasis within two years after clinical treatment [30]. Moreover, several disadvantages, including radio-resistance, toxicity and side effects, limit the use of existing standard chemo-radiation strategies. Therefore, it is urgent to explore innovative effective drugs against NPC with minimal toxicity.

Recent research has suggested that flavonoids may act as potential therapeutic agents for various types of cancer. For instance, genistein and quercetin inhibited cancer of the breasts, lungs, stomach, liver, colon, prostate, cervix and ovaries by disrupting cell proliferation, arresting cell cycle and promoting cell apoptosis [31, 32]. MA is a derivative of dihydroflavone and our previous studies showed that chloroform extract from *Sophora tonkinensis*, in which it is one of the main components, exerted excellent anti-cancer effect in NPC cells [33]. Therefore, we hypothesize that MA may exhibit an equally potent impact on NPC. It is common knowledge that proliferation and resistance to apoptosis are the major biological characteristics of malignant tumor cells [34]. In this study, we confirmed that MA inhibited cell proliferation, arrested cell cycle at $G_0/G_1$ phase and promoted the apoptosis of NPC CNE1 and CNE2 cells. CCK-8 and EdU assays showed that MA significantly reduced the survival rates of CNE1 and CNE2 cells in time- and concentration-dependent

manners. These results strongly suggested that MA acted as an effective antitumor agent for NPC patients.

The cell cycle is a biological process that controls cell proliferation and differentiation. Cyclins, cyclin-dependent kinases (CDK) and cyclin-dependent kinase inhibitors (CKIs), together form the signaling regulatory network of the cell cycle [35, 36]. Cyclin D1 and the CDK4/6 protein complex are the main regulators of $G_0/G_1$ phase. P16 and P21 are two typical CKIs that can inhibit cell cycle [37, 38]. In this study, MA increased the proportion of cells at $G_0/G_1$ phase. Western blot anaylsis also showed that MA dose dependently downregulated the expression of CDK6, CDK4 and Cyclin D1 and upregulated the expression of P21 and p16, suggesting that it can trigger the arrest of CNE1 and CNE2 cells at $G_0/G_1$ phase.

Apoptosis is the dominant mode of programmed cell death that plays an irreplaceable role in the biological process of proliferation, development, survival and death. Tumor cells have developed multiple strategies in order to evade or resist apoptosis [39, 40]. Drugs that effectively restore the normal apoptotic pathways of tumor cells have the potential to treat cancer [41]. In our study, flow cytometry results demonstrated that treatment with MA for 24 h induced apoptosis in CNE1 and CNE2 cells. In addition, Bcl-2 and the caspase family of genes play a crucial role in regulating cell apoptosis. Bcl-2 and Bax are the most important pair of molecules in Bcl-2 family. When the latter is highly expressed intracellularly, the cells are sensitive to death signals and prone to apoptosis. However, Bcl-2 plays an anti-apoptotic role by forming a heterodimer with Bax [42]. Caspase-3 is a downstream apoptotic execution molecule in both intrinsic and extrinsic cell death pathways and can initiate cell apoptosis after activation and cleavage by upstream molecules [43]. Western blot results revealed that MA up-regulated the ratios of Bax/Bcl-2 and cleaved caspase-3/total caspase-3 in a dose-dependent manner in both NPC cell lines. PARP is the downstream substrate of caspase-3 and can be cleaved by activated caspase-3 [44]. The ratio of cleaved PARP/total PARP was consistent with the above results, suggesting that MA acted as an apoptotic promoter in CNE1 and CNE2 cells. However, the pathway of MA-induced apoptosis in NPC cells remains to be further confirmed.

The mitogen-activated protein kinase (MAPK) pathway encompasses three main cascades of which the rat sarcoma (Ras)-rapidly accelerated fibrosarcoma (Raf)-mitogen-activated protein kinase kinase (MEK)-extracellular signal-regulated kinase (Erk) is one of the most dysregulated in human cancer. This pathway has a tertiary kinase mode in the signal transmission process. The small G protein, Ras, can be activated by growth factors, cytokines and proto-oncogenes, which subsequently leads to activation of the serine/threonine kinase, Raf, MEK and Erk in a cascade sequence [45]. The MAPK/Ras signaling pathway plays a pivotal role in converting extracellular stimuli into intracellular responses, including cell proliferation, differentiation, senescence, apoptosis and has long been considered to be an attractive strategy for antitumor therapies [46, 47]. In the current study, RNA-seq and KEGG pathway enrichment analysis were performed to predict possible mechanisms of the antitumor effect of MA. The results showed that the MAPK and Ras signaling pathways may play a crucial role in the action of MA. The Ras-Raf-MEK-Erk system is a common molecular approach between these two closely related signaling pathways. Western blot revealed that the phosphorylation of cRaf, MEK1/2 and Erk1/2 were blocked by MA in a dose-dependent manner. Moreover, inhibition of MA on the signal transduction pathway in NPC cell lines was rescued by the presence of TBHQ, a MAPK/Ras signaling pathway activator. The results demonstrated that MA exerted anticancer effect through suppressing the MAPK/Ras pathways. However, the accurate target of MA still needs further investigation. Furthermore, MA significantly inhibited the growth of CNE1 and CNE2 in nude mice without significant body weight loss and pathologic damage to vital organs, suggesting that this compound can be used safely *in vivo*. In addition, the results obtained from IHC staining showed that MA regulated the expression of the cell phenotype and pathway-related biomarkers, which was consistent with our findings *in vitro*.

## Conclusions

Our findings demonstrated that MA, at relatively low concentrations with minimal toxicity, exerted anti-tumor effect in NPC. MA suppressed proliferation and induce apoptosis of NPC cells by inhibiting the MAPK/Ras signaling pathway. Our study provides theoretical basis for further developing MA as a potential candidate treatment for NPC patients.

## Acknowledgments

The authors thank Dr. Dev Sooranna of Imperial College London for editing the manuscript.

## References

[1] Chen YP, Chan ATC, Le QT, *et al*. Nasopharyngeal carcinoma [J]. *J Lancet*, 2019, **394**(10192): 64-80.
[2] Sung H, Ferlay J, Siegel RL, *et al*. Global cancer statistics 2020: GLOBOCAN estimates of incidence and mortality worldwide for 36 cancers in 185 countries [J]. *CA-Cancer J Clin*, 2021, **71**(3): 209-249.
[3] Zhang B, Mo Z, Du W, *et al*. Intensity-modulated radiation therapy versus 2D-RT or 3D-CRT for the treatment of nasopharyngeal carcinoma: a systematic review and meta-analysis [J]. *Oral Oncology*, 2015, **51**(11): 1041-1046.
[4] Mao YP, Tang LL, Chen L, *et al*. Prognostic factors and failure patterns in non-metastatic nasopharyngeal carcinoma after intensity-modulated radiotherapy [J]. *Chin J Cancer*, 2016, **35**(1): 673-682.
[5] Ribassin-Majed L, Marguet S, Lee AWM, *et al*. What is the best treatment of locally advanced nasopharyngeal carcinoma? An individual patient data network meta-analysis [J]. *J Clin Oncol*, 2017, **35**(5): 498-505.
[6] Hou M, Hu W, Xiu Z, *et al*. Preparative purification of total flavonoids from *Sophora tonkinensis* Gagnep. by macroporous resin column chromatography and comparative analysis of flavonoid profiles by HPLC-PAD [J]. *Molecules*, 2019, **24**(17): 3200.
[7] Huang M, Deng S, Han Q, *et al*. Hypoglycemic activity and the potential mechanism of the flavonoid rich extract from *Sophora tonkinensis* Gagnep. in KK-Ay mice [J]. *Front Oharmacol*, 2016, **7**(151): 288.
[8] He CM, Cheng ZH, Chen DF. Qualitative and quantitative ana-

lysis of flavonoids in *Sophora tonkinensis* by LC/MS and HPLC [J]. *Chin J Nat Med*, 2013, **11**(6): 690-698.
[9] Wang CW, Chen GY, Song XP, *et al*. Flavonoids from the roots of *Millettia speciosa* Champ [J]. *Chin Tradit Pat Med*, 2014, **36**(10): 2111-2114.
[10] Fu M, Xiao G, Xu Y, *et al*. Chemical constituents from roots of *Millettia speciosa* [J]. *Chin Herb Med*, 2016, **8**(4): 385-389.
[11] Wei G, Chen Y, Guo X, *et al.* Biosyntheses characterization of alkaloids and flavonoids in *Sophora flavescens* by combining metabolome and transcriptome [J]. *Sci Rep*, 2021, **11**(1): 7388.
[12] Zhou J, Zhang L, Li Q, *et al*. Simultaneous optimization for ultrasound-assisted extraction and antioxidant activity of flavonoids from *Sophora flavescens* using response surface methodology [J]. *Molecules*, 2018, **24**(1): 112.
[13] Li P, Chai WC, Wang ZY, *et al*. Bioactivity-guided isolation of compounds from *Sophora flavescens* with antibacterial activity against *Acinetobacter baumannii* [J]. *Nat Prod Res*, 2021, **12**: 1-9.
[14] Liu XY, Zhang YB, Yang XW, *et al*. Simultaneous determination of twenty-five compounds with anti-inflammatory activity in *Spatholobi Caulis* by using an optimized UFLC-MS/MS method: an application to pharmacokinetic study [J]. *J Pharmaceut Biomed*, 2021, **204**: 114267.
[15] Lee JW, Lee JH, Lee C, *et al*. Inhibitory constituents of *Sophora tonkinensis* on nitric oxide production in RAW 264.7 macrophages [J]. *Bioorg Med Chem Lett*, 2015, **25**(4): 960-962.
[16] Lee HW, Ryu HW, Kang MG, *et al*. Potent selective monoamine oxidase B inhibition by maackiain, a pterocarpan from the roots of *Sophora flavescens* [J]. *Bioorg Med Chem Lett*, 2016, **26**(19): 4714-4719.
[17] Guo J, Li J, Wei H, *et al*. Maackiain protects the kidneys of type 2 diabetic rats *via* modulating the Nrf2/HO-1 and TLR4/NF-κB/Caspase-3 pathways [J]. *Drug Des Dev Ther*, 2021, **15**: 4339-4358.
[18] Liu Y, Zeng W, Ma C, *et al.* Maackiain dampens osteoclastogenesis *via* attenuating RANKL-stimulated NF-κB signalling pathway and NFATc1 activity [J]. *J Cell Mol Med*, 2020, **24**(21): 12308-12317.
[19] Bai X, Zhu Y, Jie J, *et al*. Maackiain protects against sepsis *via* activating AMPK/Nrf2/HO-1 pathway [J]. *Int Immunopharmacol*, 2022, **108**: 108710.
[20] Bui D, Yin T, Duan S, *et al*. Pharmacokinetic characterization and bioavailability barrier for the key active components of botanical drug antitumor B (ATB) in mice for chemoprevention of oral cancer [J]. *J Nat Prod*, 2021, **84**(9): 2486-2495.
[21] Aratanechemuge Y, Hibasami H, Katsuzaki H, *et al*. Induction of apoptosis by maackiain and trifolirhizin (maackiain glycoside) isolated from sanzukon (*Sophora Subprostrate* Chen et T. Chen) in human promyelotic leukemia HL-60 cells [J]. *Oncol Rep*, 2004, **12**(6): 1183-1188.
[22] Peng F, Wang L, Xiong L, *et al*. Maackiain modulates miR-374a/GADD45A axis to inhibit triple-negative breast cancer initiation and progression [J]. *Front Pharmacol*, 2022, **13**: 806869.
[23] Li R, Li H, Lan J, *et al*. Damnacanthal isolated from morinda species inhibited ovarian cancer cell proliferation and migration through activating autophagy [J]. *Phytomedicine*, 2022, **100**: 154084.
[24] Wang B, Gong S, Han L, *et al*. Knockdown of HDAC9 inhibits osteogenic differentiation of human bone marrow mesenchymal stem cells partially by suppressing the MAPK signaling pathway [J]. *Clin Interv Aging*, 2022, **17**: 777-787.
[25] Xia Y, Yu W, Cheng F, *et al*. Photobiomodulation with blue laser inhibits bladder cancer progression [J]. *Front Oncol*, 2021, **11**: 701122.
[26] Wingett SW, Andrews S, FastQ Screen: a tool for multi-genome mapping and quality control [J]. *F1000 Research*, 2018, **7**: 1338.
[27] Xie XT, Kropinski AM, Tapscott B, *et al*. Prevalence of fecal viruses and bacteriophage in Canadian farmed mink (Neovison vison) [J]. *MicrobiologyOpen*, 2019, **8**(1): e00622.
[28] Wei KR, Zheng RS, Zhang SW, *et al*. Nasopharyngeal carcinoma incidence and mortality in China, 2013 [J]. *Chin J Cancer*, 2017, **36**(90): 1-8.
[29] Lee HM, Okuda KS, González FE, *et al.* Current perspectives on nasopharyngeal carcinoma [J]. *Adv Exp Med Biol*, 2019, **1164**: 11-34.
[30] Lee AW, Ma BB, Ng WT, *et al*. Management of nasopharyngeal carcinoma: current practice and future perspective [J]. *J Clin Oncol*, 2015, **33**(29): 3356-3364.
[31] Sharifi-Rad J, Quispe C, Imran M, *et al.* Genistein: an integrative overview of its mode of action, pharmacological properties, and health benefits [J]. *Oxid Med Cell Longev*, 2021, **2021**: 3268136.
[32] Almatroodi SA, Alsahli MA, Almatroudi A, *et al*. Potential therapeutic targets of quercetin, a plant flavonol, and its role in the therapy of various types of cancer through the modulation of various cell signaling pathways [J]. *Molecules*, 2021, **26**(5): 1315.
[33] Wang S, Song Z, Gong X, *et al.* Chloroform extract from *Sophora tonkinensis* Gagnep. inhibit proliferation, migration, invasion and promote apoptosis of nasopharyngeal carcinoma cells by silencing the PI3K/AKT/mTOR signaling pathway [J]. *J Ethnopharmacol*, 2021, **271**: 113879.
[34] Hanahan D, Weinberg RA, Hallmarks of cancer: the next generation [J]. *Cell*, 2011, **144**(5): 646-674.
[35] Matthews HK, Bertoli C, de Bruin RAM, Cell cycle control in cancer [J]. *Nat Rev Mol Cell Bio*, 2022, **23**(1): 74-88.
[36] Suski JM, Braun M, Strmiska V, *et al*. Targeting cell-cycle machinery in cancer [J]. *Cancer Cell*, 2021, **39**(6): 759-778.
[37] Goel S, Bergholz JS, Zhao JJ. Targeting CDK4 and CDK6 in cancer [J]. *Nat Rev Cancer*, 2022, **22**: 356-372.
[38] Fassl A, Geng Y, Sicinski P, CDK4 and CDK6 kinases: from basic science to cancer therapy [J]. *Science*, 2022, **375**(6577): eabc1495.
[39] Hanahan D, Hallmarks of cancer: new dimensions [J]. *Cancer Discov*, 2022, **12**(1): 31-46.
[40] Zhang Y, Qu Y, Chen YZ, Influence of 6-shogaol potentiated on 5-fluorouracil treatment of liver cancer by promoting apoptosis and cell cycle arrest by regulating AKT/mTOR/MRP1 signalling [J]. *Chin J Nat Med*, 2022, **20**(5): 352-363.
[41] Carneiro BA, El-Deiry WS. Targeting apoptosis in cancer therapy [J]. *Nat Rev Clin Oncol*, 2020, **17**(7): 395-417.
[42] Hata AN, Engelman JA, Faber AC, The BCL2 family: key mediators of the apoptotic response to targeted anticancer therapeutics [J]. *Cancer Discov*, 2015, **5**(5): 475-487.
[43] Haider T, Tiwari R, Vyas SP, *et al*. Molecular determinants as therapeutic targets in cancer chemotherapy: an update [J]. *Pharmacol Therapeut*, 2019, **200**: 85-109.
[44] Dias MP, Moser SC, Ganesan S, *et al*. Understanding and overcoming resistance to PARP inhibitors in cancer therapy [J]. *Nat Rev Clin Oncol*, 2021, **18**(12): 773-791.
[45] Dillon M, Lopez A, Lin E, *et al*. Progress on Ras/MAPK signaling research and targeting in blood and solid cancers [J]. *Cancers*, 2021, **13**(20): 5059.
[46] Sebolt-Leopold JS, Herrera R. Targeting the mitogen-activated protein kinase cascade to treat cancer [J]. *Nat Rev Cancer*, 2004, **4**(12): 937-947.
[47] Jing SY, Wu ZD, Zhang TH, *et al*. *In vitro* antitumor effect of cucurbitacin E on human lung cancer cell line and its molecular mechanism [J]. *Chin J Nat Med*, 2020, **18**(7): 483-490.

**Cite this article as:** JIANG Xing, YANG Xiaonan, SHI Yanxia, LONG Yan, SU Wenqing, HE Wendong, WEI Kunhua, MIAO Jianhua. Maackiain inhibits proliferation and promotes apoptosis of nasopharyngeal carcinoma cells by inhibiting the MAPK/Ras signaling pathway [J]. *Chin J Nat Med*, 2023, **21**(3): 185-196.